China Geology 7 (2024) 747−761

China Geology

Journal homepage: http://chinageology.cgs.cn
https://www.sciencedirect.com/journal/china-geology

Sedimentary environment and organic matter accumulation of Wufeng-Longmaxi shales, southwest Yangtze Plate, China: Insights from geochemical and petrological evidence

An-kun Zhao[a, b], Dong Wang[a, b,*], Qian Zhang[a, b,*], Zi-hui Lei[b, c], Qian Yu[a, b], Di Zhang[a, b], Ye-xin Zhou[a, b]

[a] *Chengdu Center of China Geological Survey*, *Ministry of Natural Resources*, *Chengdu* 610081, *China*
[b] *Key Laboratory of Sedimentary Basin and Oil and Gas Resources*, *Ministry of Natural Resources*, *Chengdu* 610081, *China*
[c] *The College of Literature and Journalism of Sichuan University*, *Chengdu* 610064, *China*

ARTICLE INFO

Article history:
Received 4 July 2021
Received in revised form 20 September 2022
Accepted 26 September 2022
Available online 9 November 2022

Keywords:
Shales
Shale gas
Sedimentary environment
Graptolite
Upper Ordovician–Lower Silurian
Organic matter accumulation
Radiolarian
Geochemical and petrographic evidence
Wufeng-Longmaxi Formation
Oil-gas exploration engineering
Suboxic environment
Sichuan Basin
Reduced environment
Yangtze Plate

ABSTRACT

Upper Ordovician–Lower Silurian Wufeng-Longmaxi Formation is the most developed strata of shale gas in southern China. Due to the complex sedimentary environment adjacent to the Kangdian Uplift, the favorable area for organic-rich shale development is still undetermined. The authors, therefore, focus on the mechanism of accumulation of organic matter and the characterization of the sedimentary environment of the Wufeng-Longmaxi Shales to have a more complete understanding and new discovering of organic matter enrichment and favorable area in the marginal region around Sichuan Basin. Multiple methods were applied in this study, including thin section identification, scanning electron microscopy (SEM) observations and X-ray diffraction (XRD), and elemental analysis on outcrop samples. Five lithofacies have been defined according to the mineralogical and petrological analyses, including mudstone, bioclastic limestone, silty shale, dolomitic shale, and carbonaceous siliceous shale. The paleo-environments have been reconstructed and the organic enrichment mechanism has been identified as a reduced environment and high productivity. The Wufeng period is generally a suboxic environment and the early Longmaxi period is a reducing environment based on geochemical characterization. High dolomite content in the study area is accompanied by high TOC, which may potentially indicate the restricted anoxic environment formed by biological flourishing in shallower water. And for the area close to the Kangdian Uplift, the shale gas generation capability is comparatively favorable. The geochemical parameters implied that new favorable areas for shale gas exploration could be targeted, and more shale gas resources in the mountain-basin transitional zone might be identified in the future.

1. Introduction

In the last decade, the shale of the Upper Ordovician–Lower Silurian Wufeng-Longmaxi Formation in the Upper Yangtze Plate of China attracted the most attention because of its huge exploration and development potential for shale gas. Several studies have been conducted in many aspects and have attempted to gain a better understanding of the main factors influencing organic matter enrichment (Hao F and Zou HY, 2013; Zou CN et al., 2014, 2015, 2019; Pan SQ et al., 2015; Dai JX et al., 2016; Dong DZ et al., 2016; Chen XJ et al., 2022; Zhao L et al., 2023; Guo X et al., 2022). In general, organic matter enrichment is related to many factors, such as sea level fluctuations, seawater stratification, biological extinction, and boom (Lalonde K et al., 2012; Hackley PC, 2016; Nitzer SF et al., 2016; Ma YQ et al., 2016; Wang S et al., 2016; Knapp LJ et al., 2017; Li YF et al., 2017; Li SZ et al., 2022; Tang X et al., 2017; Cavelan A et al., 2019; Tserolas P et al., 2019; Zhao AK et al., 2021; Zou CN et al., 2019). Key control factors for organic matter enrichment may vary significantly in different sediment environments. It is important to examine the indices of the sedimentary environment such as paleo-productivity, hypoxia

First author: *E-mail address*: zakly@qq.com (An-kun Zhao).

* Corresponding author: *E-mail address*: wwwdong1222@qq.com (Dong Wang); 76517507@qq.com (Qian Zhang).

Literary editor: Li-qiong Jia
doi:10.31035/cg2022074
2096-5192/© 2024 China Geology Editorial Office.

environment, and detrital terrigenous input (Tribovillard N et al., 2006; Zhou L et al., 2015; Hammes U et al., 2016; Jia AL et al., 2016). Slow sedimentation rates caused by high sea levels are favorable for organic matter accumulation. Oxygen-deficiency environment could have better organic matter preservation as several studies demonstrated that organic matter content was prolific in an anoxic environment (Bernard S and Horsfield B, 2014; Tan JQ et al., 2014; Zou CN et al., 2014). High paleo-productivity like phytoplankton prosperous gives a great contribution to the organic matter accumulation, and the decomposition of the enhanced surface oceanic organic matter productivity needs higher oxygen consumption, thus resulting in an oxygen deficiency environment (Caplan and Marc, 1998; Kuypers et al.,2002).

Recently, with the increasing attention paid by scholars to the basin-mountains transitional zone around the upper Yangtze and a number of successful shale gas wells had been drilled in this area, the exploration potential has been more and more noticed. However, because of its complex sedimentary environment around the Yangtze Plate, the lithology, the sedimentary facies, and the mechanism of enrichment of organic matter vary considerably. A detailed study is necessary to conduct to have a better understanding of organic matter enrichment.

In this study, the Wufeng-Longmaxi shale in the southwest Yangtze Plate has been studied through petrological, mineralogical and a combination of independent geochemical proxies data examination from the Jiaodingshan Outcrop (JDP), east of Kangdian Uplift, south China. Multiple techniques have been applied including thin section identification, scanning electron microscope (SEM) observations, X-ray diffraction (XRD), and elemental analysis. The integrated analysis mentioned above would be useful for quantitatively characterizing the detrital influx, redox conditions, and paleo-productivity, summarizing the lithofacies, reconstructing the paleo-environments of the Upper Yangtze Plate, and supporting the global comparison by using graptolite zone as an isochronal stratigraphic framework.

2. Geological setting

The study area is located in the basin-mountain transitional zone of the southwest margin of the Yangtze Plate. During the Late Ordovician–Early Silurian period, influenced by the Caledonian movement, the study area was surrounded by Chengdu Uplift, Kangdian Uplift, and Qianzhong Uplift (Fig. 1). The sedimentary environment was mainly restricted to the marine shelf (Zou CN et al., 2019; Li SZ et. al., 2022; Yuan K et al., 2023).

The Wufeng Formation was deposited in a shallow-water platform environment with a thickness of 2–5 m (Ge XY et al., 2019). The lithology of the Wufeng Formation is dominated by manganiferous bioclastic limestone, mixed with black carbonaceous shale, rich in fossils, such as graptolite, brachiopods, conodon spines, Chitinozoa and so on (Fan JX and Chen X, 2007).

The stratigraphic contact relationship between Wufeng and Longmaxi Formations is still controversial. Some scholars believe that the strata are unconformable contacts with evidence of basal erosion(Tang JQ et al., 2017). However, no direct evidence of sedimentary discontinuity was found in the outcrop in this study. The strata of the Longmaxi Formation are shelf facies (Ge XY et al., 2019; Zhao AK et al., 2022). The lithology of its lower part is mainly siliceous and carbonaceous mudstone interlayered with pyrite beddings. Fossils like graptolite and radiolarians developed. The lithology in the upper part is dominated by carbonaceous calcareous mudstone and calcareous silty mudstone. The content of siliceous and carbonaceous mudstone gradually decreases from the bottom up, while the content of calcareous sand gradually increases upwards.

3. Samples and experiments

3.1. Samples

All 34 outcrop samples were collected from Wufeng-Longmaxi shale in the southwest of the Sichuan Basin, including 34 samples for thin section identification and SEM, 27 samples for geochemical analysis, 16 samples for organic carbon isotope tests, and 18 samples for graptolite zonation

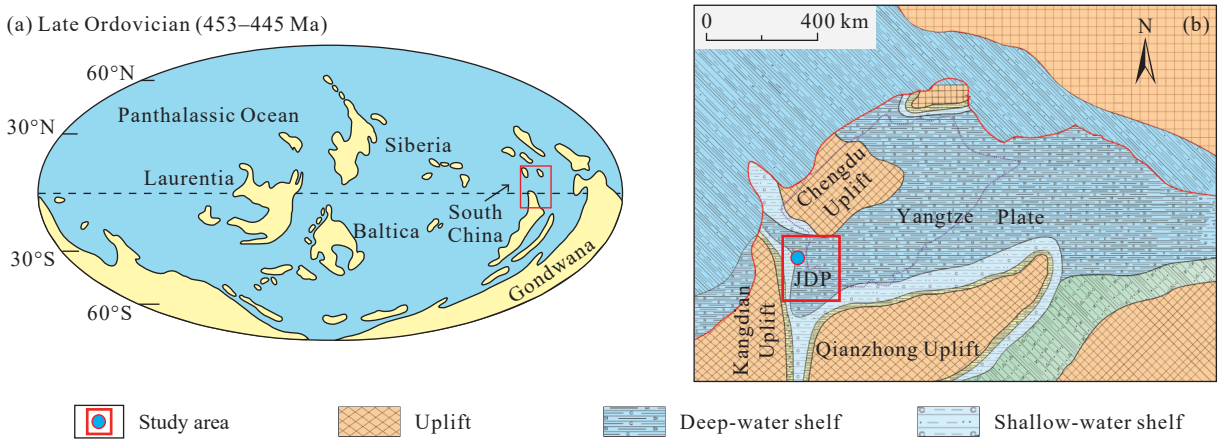

Fig. 1. a–Latest Ordovician paleogeographic maps of the world (base map after Torsvik T and Cocks L, 2016). a– paleogeographic map of the Yangtze Plate during the Late Ordovician (after Chen X et al., 2004; Liu ZH et al., 2017).

(Fig. 2). All rock samples collected are fresh and free of alteration to minimize contamination to ensure the test accuracy.

3.2. Experiments

The experiments were carried out by the Key Laboratory for Sedimentary Basin and Oil & Gas Resources of the Chengdu Center of China Geological Survey, and the Sichuan Institute of Coal Geological Engineering Design & Research, China. The following experiments and trials were conducted by the research team during the study.

The thin section identification was conducted by polished rock samples with Zeiss Scope, A1microscope. SEM Samples were prepared with a GATAN-685 argon ion mill and imaged using a QuantaTM 250 SEM.

The mineralogy of the 27 samples was studied by Bruker®X-ray Diffractometer with the shale grounded to less than 200 mesh, and the data were obtained with 0.02º per step in 3º per minute. And the TOC contents were measured with a Leco® CS-230CH Carbon/Sulfur analyzer. All the samples have been crushed and grounded to less than 100 mesh, and the carbonates in the shale were removed by hydrochloric acid digestion. After drying in an oven, 0.1 g of each sample was combusted and tested in the analyzer.

The major element analyses are conducted on Axios mAx X-ray fluorescence spectrometer with fresh sample grounded less than 200 mesh. The analysis error is less than 1 %. The test process includes weighting 0.7000 g of the sample accurately and adding a mixture of 5.2 g anhydrous lithium borate, 0.400 g lithium fluoride, 0.3 g ammonium nitrate, and 1 mL of lithium bromide. After melting samples at 1150°C, the samples were measured on the machine after casting at a temperature of 800°C.

The trace and rare earth elements were tested by ICP-MS ICAP-RQ. 100 mg samples were taken and dissolved in acid solution(1 mL HF+ 0.5 mL HCL +6 mL HNO_3) in a microwave digestion container. The temperature was set above 200°C, then the sample was evaporated and the residual samples were dissolved into the chloroazotic acid for the test.

Organic carbon isotope analysis was conducted by MS EA-Isolink-Delta V Plus. The sample (about 250–800 g) was fully combusted in the reaction tube at 960°C to generate CO_2 gas for testing. The carrier gas was helium with gas flow rates of 100 mL/min.

4. Results

4.1. Mineralogy

The mineral content of Wufeng-Longmaxi shale in the study area is significantly different vertically (Fig. 3).

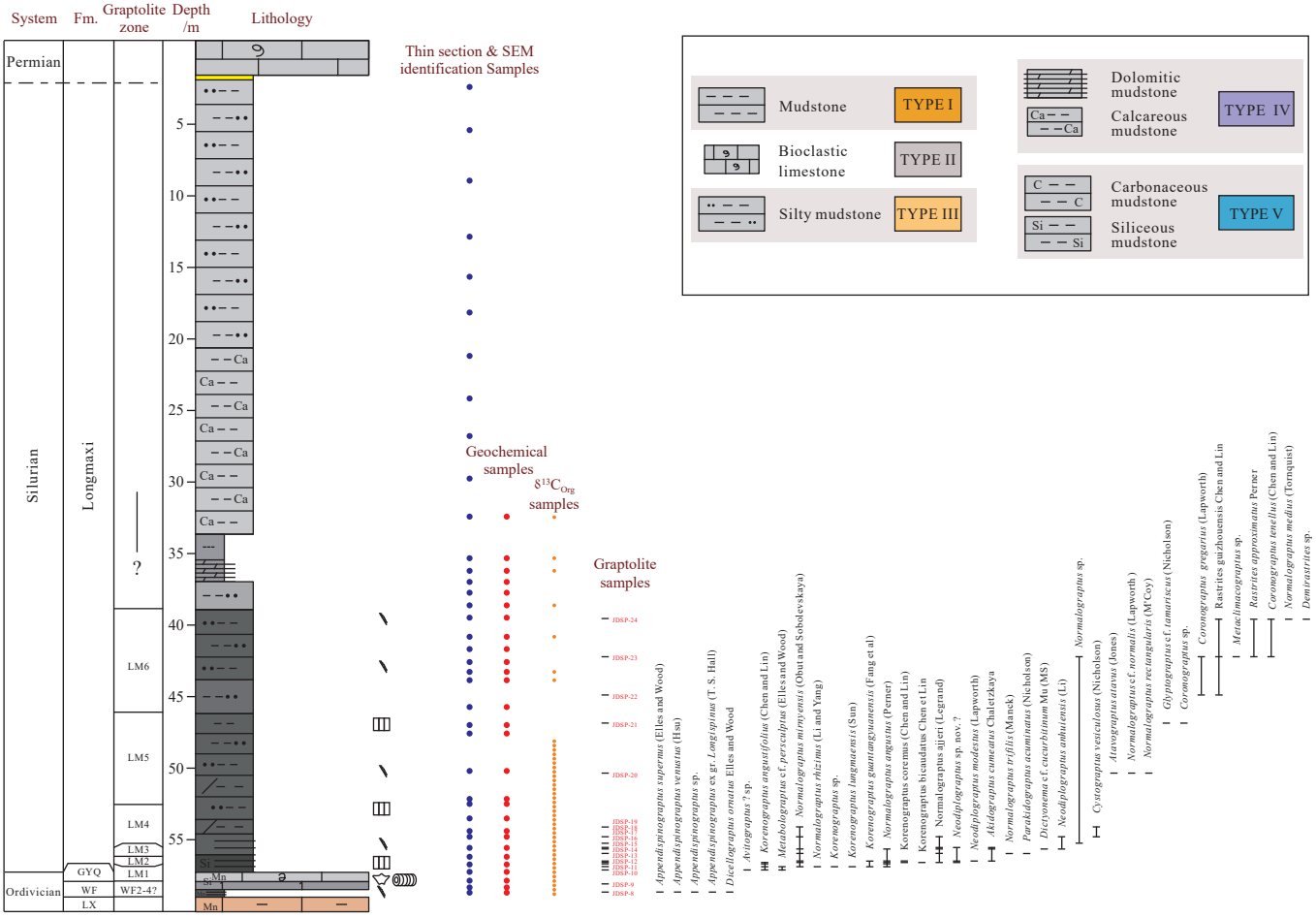

Fig. 2. Stratigraphic profile of the Wufeng-Longmaxi succession exposed in the JDP outcrop showing lithology, sample location, and stratigraphic distributions of graptolites (after Zhao AK et. al., 2022).

Stratigraphic profiles manifest the mineral content of the Wufeng Formation is mainly carbonate while the lithology of Longmaxi Formation is quartz and feldspar prevailing, with a small fraction of carbonate rocks and clay minerals. According to the mineral content, the Wufeng Formation could be subdivided into two members from the bottom up. The lower member mainly consists of manganese shale and siliceous mudstone, the upper member mainly consists of bioclastic limestone. The Longmaxi Formation could be subdivided into three parts, which are siliceous shale and dolomitic shale at the bottom, carbonaceous siliceous shale in the middle, and silty mudstone at the upper part (Fig. 4; Table 1).

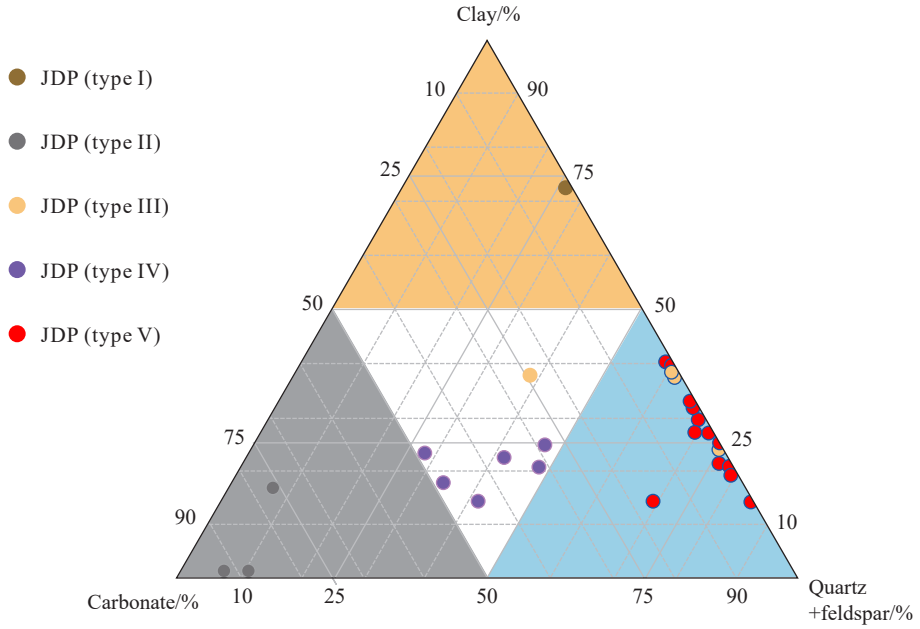

Fig. 3. Ternary diagram of the mineralogic composition of five major lithofacies from Wufeng to Longmaxi Formations in the study area (modified from Ma YQ et al., 2016).

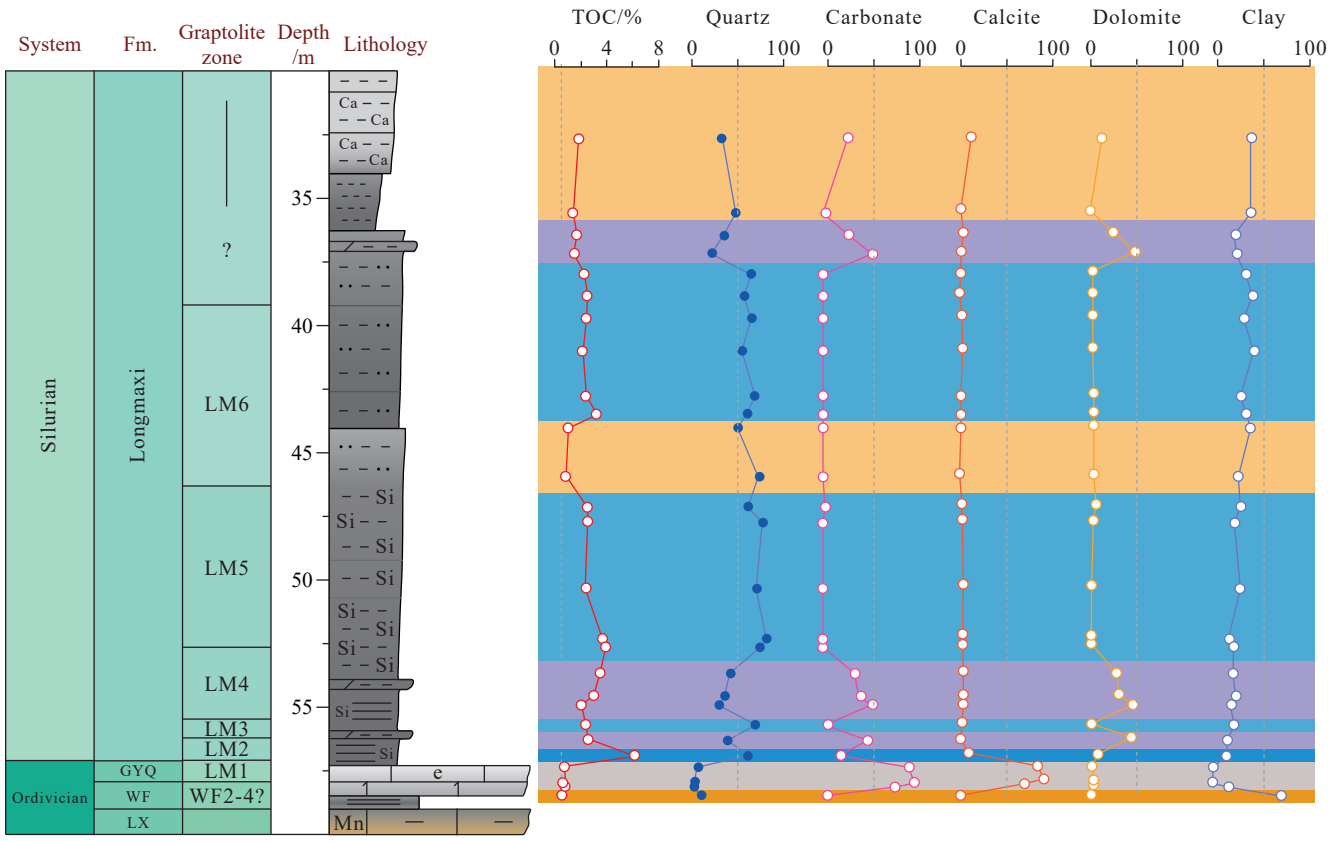

Fig. 4. Stratigraphic profile of the Wufeng-Longmaxi succession exposed in the JDP outcrop showing mineral content. The legend of the lithology is as same as Fig. 2.

Table 1. Main mineral content of the Wufeng-Longmaxi Formation in the JDP profile.

Sample No.	Quartz/ %	Feldspar/ %	Calcite/ %	Dolomite/ %	Pyrite/ %	Clay/ %
JDP-27	35	2	12	12	2	37
JDP-26	48	12	0	0	0	37
JDP-25	36	4	3	22	2	21
JDP-24	24	4	1	47	1	23
JDP-23	63	5	0	0	0	32
JDP-22	56	5	0	0	0	39
JDP-21	63	7	0	0	0	30
JDP-20	54	6	0	0	0	40
JDP-19	67	6	0	0	0	27
JDP-18	58	9	0	0	0	33
JDP-17	50	13	0	0	0	37
JDP-16	70	5	0	0	0	25
JDP-15	60	11	0	2	0	27
JDP-14	74	4	0	0	0	21
JDP-13	68	5	0	0	0	27
JDP-12	78	7	0	0	0	15
JDP-11	72	8	0	0	0	20
JDP-10	42	5	3	28	2	20
JDP-9	37	3	2	33	3	22
JDP-8	31	1	0	47	4	17
JDP-7	68	8	2	0	1	21
JDP-6	40	0	0	44	2	14
JDP-5	60	7	9	7	3	14
JDP-4	10	0	84	0	3	0
JDP-3	7	0	90	0	3	0
JDP-2	6	0	70	0	9	15
JDP-1	14	11	0	0	4	67

According to the lithofacies classification by outcrop and thin section observations, and mineral and TOC content (Han C et al., 2016), Wufeng-Longmaxi shale in the study area had been divided into five lithofacies (Fig. 4). Type Ⅰ: Mudstone (clay content over 50%); Type Ⅱ: Bioclastic limestone (carbonate content over 50%); Type Ⅲ: Silty shale (silt content over 25%); Type Ⅳ: Dolomitic shale (siliceous over 50%, carbonate between 25% and 50%); Type Ⅴ: Carbonaceous siliceous shale (siliceous over 50%, the TOC over 2%).

4.2. Petrological characteristics

According to the petrographic classification mentioned above, the petrological characteristics of the five lithofacies were observed in detail in macroscopic, hand specimens, and under the microscope. Type I thin layer shale at the bottom of the Wufeng Formation is rich in clay minerals, and the clay mineral content is more than 70%. Type II manganese-bearing bioclastic limestone is located in the middle and upper part of the Wufeng Formation. The bioclasts are mainly crustaceans, and some of the body cavities were filled with calcite. A large number of pyrite nodules (Fig. 5e) can be seen in the layer. Macroscopically, the hand specimen was found to be rich in bioclasts, and the organism burrows (Fig. 5f) were seen on the outcrop level. The bottom and middle-lower part of the Longmaxi Formation are mainly Type V siliceous carbonaceous shale (Fig. 5d, g), rich in graptolite (Fig. 5a), intercalated with several layers of porphyry, and calcareous nucleation (Fig. 5b) is seen in the layer. Microscopically siliceous fossils such as radiolaria (Fig. 6f), spongy bone needles, and strawberry-like pyrite (Fig. 6c) are visible. The type IV dolomitic shale (Fig. 6d) is sandwiched between them, and the crystalline form of dolomite particles is better under the microscope (Fig. 6e). Type III silty mudstone developed in the upper part of the Longmaxi Formation and is not fully outcropped.

4.3. Geochemical characteristics

The content of the paleo-productivity index Ba changed greatly, the value was 0.038%–1.80%, and the average value was 0.40%; P content was 0.017%–0.36 %, and the average value was 0.054%. The P content in Wufeng Formation showed a high value, but the P content in Longmaxi Formation did not change much. The biogenic silica content

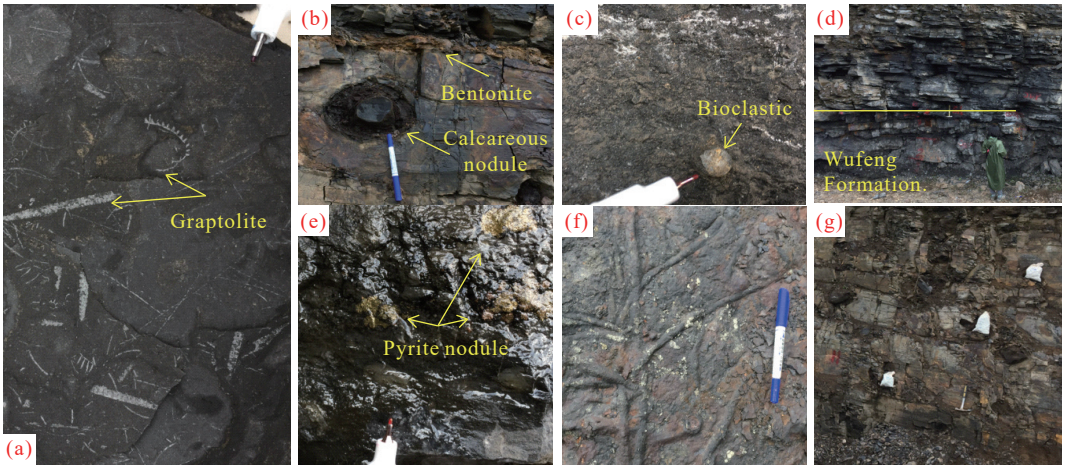

Fig. 5. Outcrop of Wufeng-Longmaxi Formation in the JDP. a–abundant graptolite fossils; b–calcareous nodules and bentonite intercalation in the shale; c–bioclasts in Wufeng Formation; d–macroscopic characteristics of Wufeng and Longmaxi Formations; e–pyrite nodules in Wufeng Formation; f–bio remains in the top of Wufeng Formation; g–sampling location of siliceous shale.

(SiO_{2bio}) value was 0%–10% in Wufeng Formation, while was 20%–70.7% in Longmaxi Formation, and the average value was 36.5%, showing a low value in Wufeng Formation (Fig. 7). While the siliceous biological content in the lower part of the Longmaxi Formation was higher, showing a trend of slow decrease. However, Mn content was 0.01%–13.95%, and the average value was 1.08% (Table 2). The Wufeng Formation showed an extremely high value of Mn, which corresponded to the manganite deposit in the Wufeng period of this area. The manganese content in the lower part of the Longmaxi Formation was relatively high, and the manganese content in the upper part of the Longmaxi Formation changed

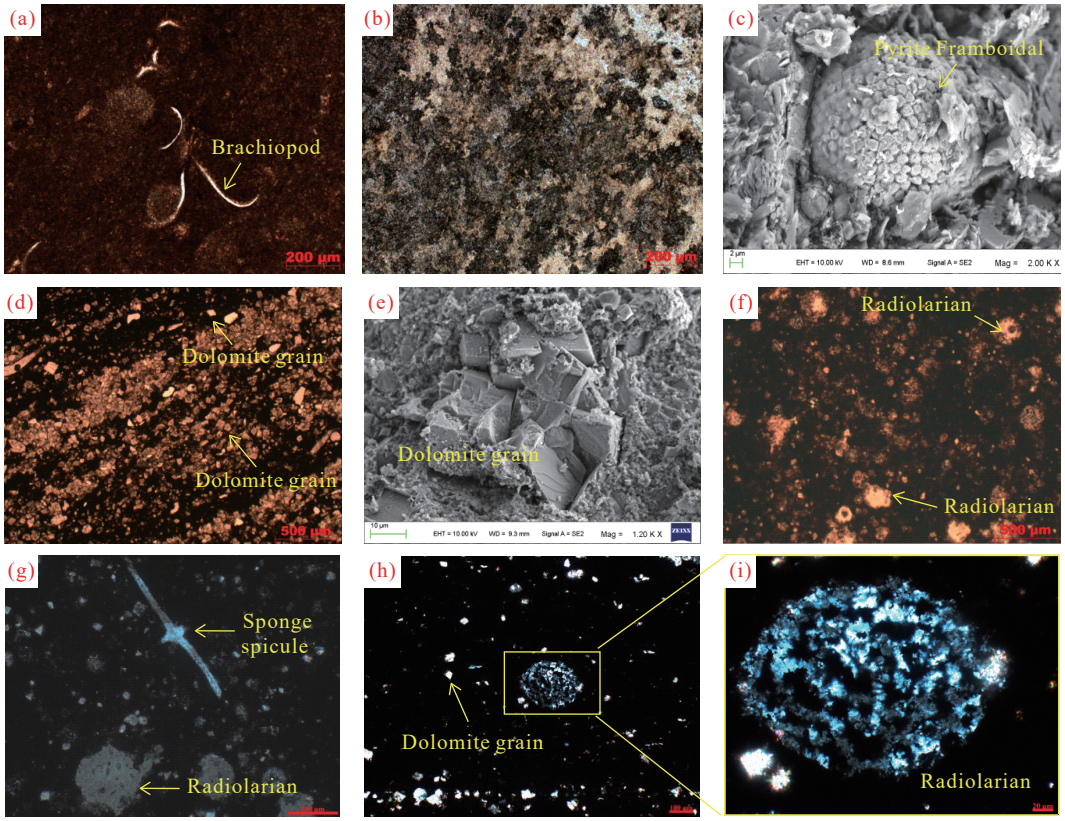

Fig. 6. Microscope and SEM images of Wufeng-Longmaxi Formation in the JDP. a–crustaceans bioclasts were replaced by calcite filling; b–micrite with micritic structure, calcite about 70%; c–SEM strawberry pyrite particles; d–dolomitic mudstone, dolomite d distribution in bands; e–SEM dolomite particles; f–bioclasts are mainly radiolarian, circular or elliptical distribution, replaced by carbonate components; g–radiolarians and sponge spicule; h, i–dolomite grain and radiolarians.

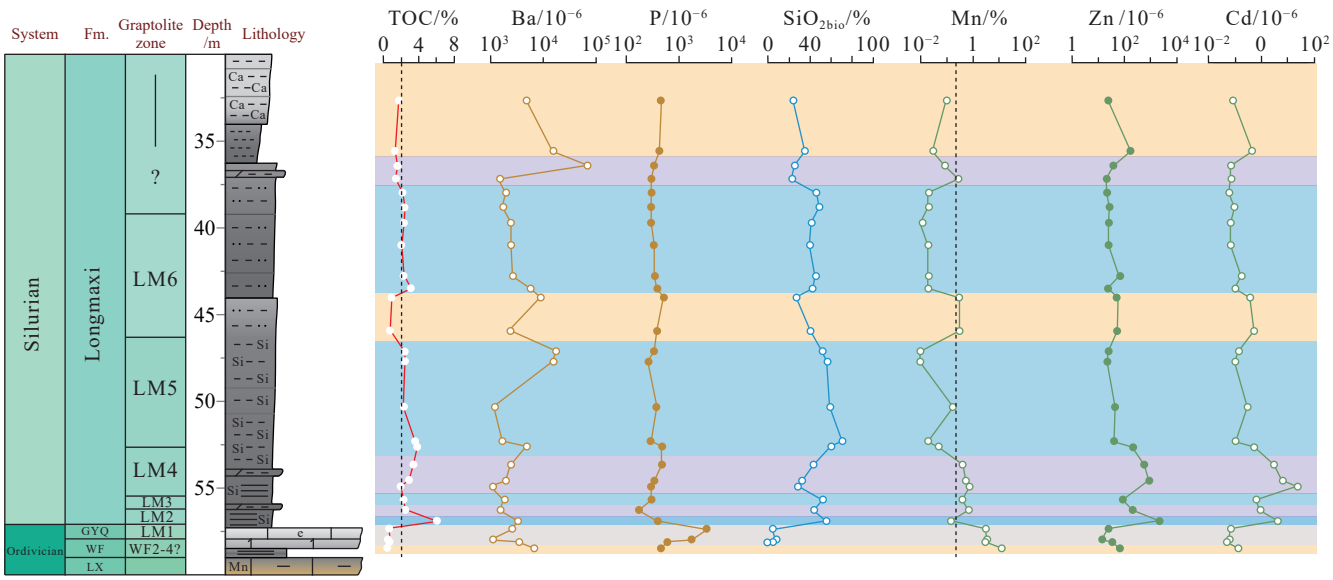

Fig. 7. Stratigraphic profile of the Wufeng-Longmaxi succession exposed in the JDP outcrop of paleo-productivity (TOC and Mn data from Zhao AK et. al., 2022).

Table 2. Geochemical proxies of the Wufeng-Longmaxi Formation in the JDP profile.

Sample No.	Al_2O_3/%	Ti%	V/Cr	Ni/Co	Mn/%	Zn/10^{-6}	Cd/10^{-6}	Ba/%	P/%	Si/%	Th/U	δ^{13}Corg $_{V\text{-}PDB}$/‰
JDP-27	11.20	0.29	2.28	4.90	0.10	25.70	0.09	5014.38	480.28	24.41	1.98	−29.56
JDP-26	13.05	0.37	1.81	4.13	0.03	190.80	0.49	15759.48	436.62	35.65	1.98	−28.53
JDP-25	9.33	0.39	1.81	5.07	0.09	41.30	0.07	74499.35	349.30	25.57	2.06	−29.02
JDP-24	9.24	0.23	2.18	5.34	0.30	21.60	0.07	1432.68	305.63	22.58	1.95	-
JDP-23	11.03	0.26	1.77	4.71	0.02	23.00	0.06	1969.93	305.63	46.79	2.04	-
JDP-22	10.78	0.26	1.87	6.83	0.02	29.00	0.10	1701.31	305.63	49.53	1.97	−28.9
JDP-21	12.33	0.30	1.93	7.21	0.01	26.60	0.07	2507.19	305.63	41.69	1.84	
JDP-20	12.84	0.29	1.68	5.90	0.02	26.80	0.07	2507.19	349.30	40.00	2.47	−28.75
JDP-19	11.35	0.28	1.85	6.26	0.02	68.00	0.18	2686.27	349.30	45.44	1.82	-
JDP-18	11.85	0.29	1.84	5.17	0.02	25.40	0.10	5909.80	392.96	43.25	1.26	−28.75
JDP-17	15.21	0.43	1.84	6.61	0.33	62.50	0.39	9222.88	523.94	27.21	1.83	−28.16
JDP-16	12.69	0.35	1.95	6.66	0.33	58.60	0.56	2328.10	392.96	40.73	1.53	-
JDP-15	8.67	0.25	1.98	4.88	0.01	26.00	0.14	18266.67	349.30	51.79	1.39	-
JDP-14	8.34	0.23	2.11	5.25	0.01	23.70	0.10	15938.56	261.97	56.63	1.31	−29.28
JDP-13	7.85	0.20	3.64	4.76	0.19	48.00	0.31	1164.05	392.96	59.44	0.40	−29.43
JDP-12	5.21	0.14	2.96	6.72	0.02	43.70	0.11	1701.31	305.63	71.42	0.40	-
JDP-11	6.97	0.20	3.43	8.29	0.05	215.40	0.58	4924.84	480.28	60.54	0.20	-
JDP-10	6.61	0.19	3.45	8.84	0.45	627.90	3.29	2417.65	480.28	43.59	0.33	-
JDP-9	5.96	0.18	3.90	5.96	0.57	941.80	6.55	1969.93	349.30	32.89	0.31	−29.94
JDP-8	4.37	0.12	3.83	5.60	0.82		24.55	626.80	305.63	29.19	0.40	-
JDP-7	5.10	0.12	3.31	7.44	0.42	93.50	0.66	1790.85	305.63	52.63	0.28	−30.11
JDP-6	3.51	0.10	5.50	9.03	0.72	227.80	0.92	1522.22	174.65	44.04	0.27	−30.28
JDP-5	5.28	0.16	16.06	12.46	0.16		4.54	3402.61	392.96	55.77	0.23	−30.44
JDP-4	3.05	0.12	4.92	0.85	3.22	25.40	0.07	2596.73	3623.94	4.45	0.52	−29.41
JDP-3	1.91	0.06	3.76	1.15	3.70	14.60	0.06	447.71	1833.80	7.38	0.17	-
JDP-2	3.00	0.10	3.05	0.60	3.56	36.90	0.05	3313.07	611.27	3.56	1.10	−29.24
JDP-1	13.40	0.35	4.42	0.65	13.95	71.00	0.14	7342.48	480.28	-4.32	1.64	−28.87

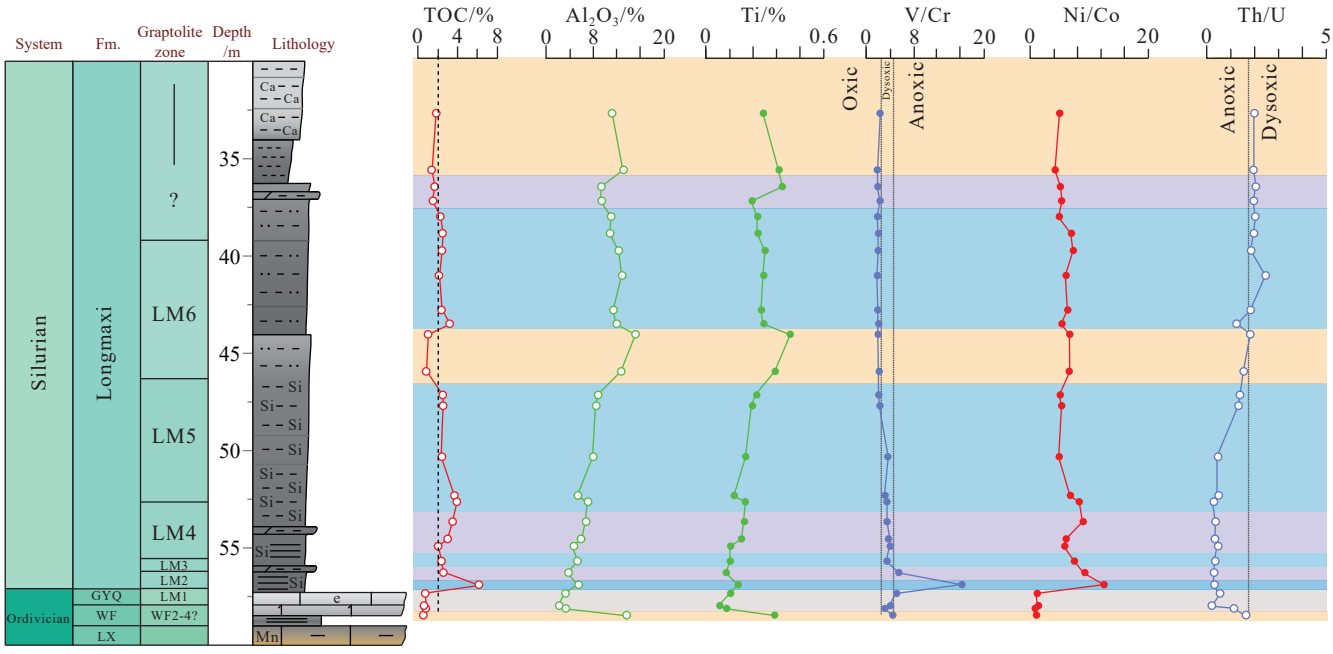

Fig. 8. Stratigraphic profile of the Wufeng-Longmaxi succession exposed in the JDP outcrop showing terrigenous influx and redox environment (V/Cr and Al_2O_3 data from Zhao AK et. al., 2022).

greatly and showed a good correlation. Generally speaking, the manganese content of Wufeng was lower, and the bottom of the Longmaxi Formation showed a high value.

The terrestrial detrital indices of Al_2O_3 and Ti had a good correlation in the study area. Al_2O_3 content was 3%–15.21%, and the average value was 8.52 % (Table 2). The overall Ti content changed little and the value was 6.6%–0.43 %, and the average value was 0.23%. The Al_2O_3 content showed a

low value in Wufeng Formation, indicating that the amount of terrestrial detrital input in the Wufeng period was less, and the value increased at first and then decreased during the Guanyinqiao period, indicating that the terrestrial detrital input was larger during the Guanyinqiao period. The whole Longmaxi Formation shows a trend of increasing gradually, then decreasing and increasing again, with less terrestrial detrital input at the bottom and a high value of terrestrial detrital input in the middle part, with an average of about 14%. The whole terrestrial debris in the Longmaxi period increases gradually.

The redox index parameters V/Cr and Ni/Co have a good correlation. The Wufeng Formation is in the sub-oxygen environment as a whole, and the bottom of the Longmaxi formation shows the highest value, showing a transient strong reduction environment, and then rapidly becomes a sub-oxidation environment. The overall trend of oxidation increases gradually, indicating that the water body gradually becomes shallower, and the redox index Th/U shows a similar trend, indicating that the Wufeng Formation is in the sub-oxidation environment. The Longmaxi period is an environment in which the oxidization is gradually enhanced.

5. Discussion

5.1. Sedimentary environment of Wufeng-Longmaxi shale

The sedimentary environment plays an important role in the organic matter accumulation, which influences the organic-rich shale quality. In general, the influence of the sedimentary environment on the formation of organic-rich shale is discussed by the input of terrigenous detrital, the redox environment of a water body, and the paleo-productivity index. Thus, a combination of independent geochemical proxies is used to determine the redox state of the bottom water. The clastic input is evaluated based on the Al_2O_3 (%) and titanium (Ti) contents. The SiO_{2bio}, Ba, P, Mn, Zn, and Cd proxies are used for primary productivity evaluation.

5.1.1. Terrigenous influx

Generally, the content of Al_2O_3 and TiO_2 increases with the continuous input of terrestrial materials, and the content is relatively stable, rarely affected by diagenesis or metamorphism even later, so it could be used to discuss the influence index of detrital material input on organic matter enrichment (Murray et al., 1990). The column of Al_2O_3 and TiO_2 exhibits similarly an increasing trend of terrigenous input from the bottom up (Fig. 8). From the stratigraphic profile, the terrigenous influx gradually increases upwards. Mudstone (Type I) and silty mudstone (Type III) have the highest terrigenous influx, while dolomitic mudstone (Type IV) have less terrigenous influx and siliceous shale (Type V) has a minimum value. For limestone (Type II), there is little terrigenous material input as the sedimentary facies for it is carbonate platforms deposits.

5.1.2. Redox environment

The redox environment of the water column is one of the main controlling factors for the preservation of organic matter. Numerous studies manifested that V, Cr, Th, Co, Ni, Mo, and U are enriched in reducing sedimentations, and could be used as indicators of redox conditions (Ma YQ et. Al., 2016). Vanadium may be bound to organic matter by the incorporation of V^{4+} into porphyrins , thus, high content of element V in sediments usually indicates reduction environment, and V/Cr could be used as an indicator of an anoxic environment. The Ni would form sulfide precipitates with H_2S in a reducing environment while it exists in an ionic form in an oxidizing environment. Co would be dissolved in water as Co^{2+} in an oxidizing environment or trapped in the

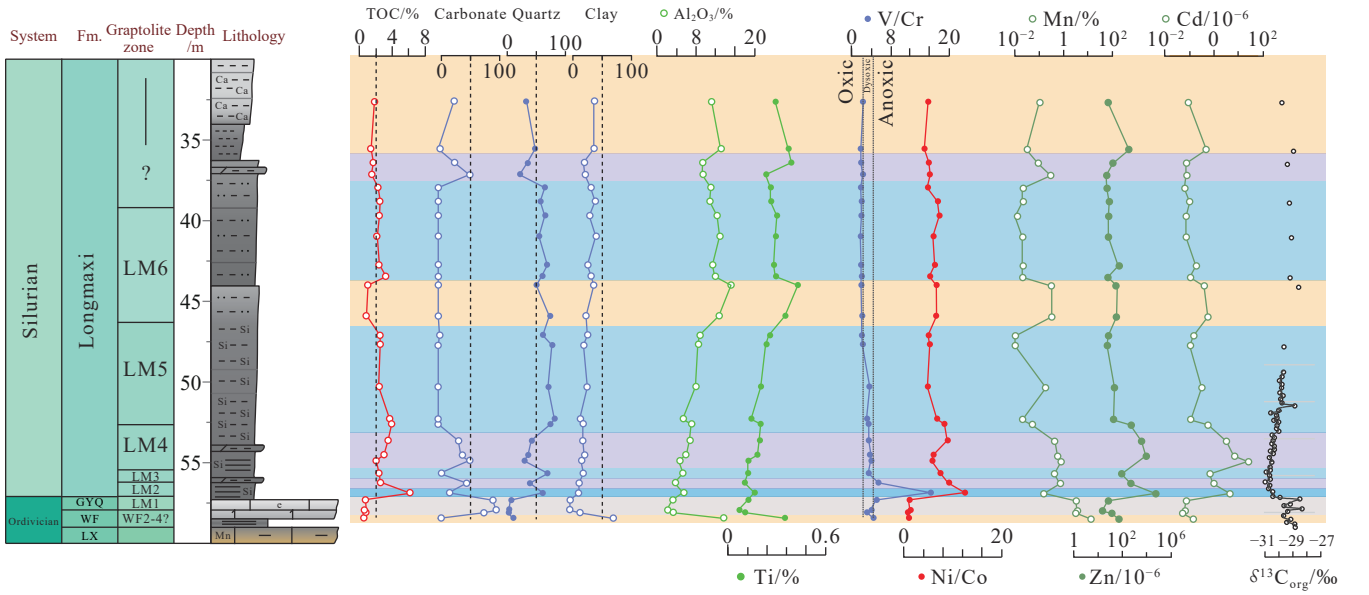

Fig. 9. Comprehensive profile of the Wufeng-Longmaxi succession exposed in the JDP outcrop showing total organic matter, and geochemical data of redox conditions, productivity, and detrital input.

authigenic pyrite in an anoxic environment. Thus, Ni/Co can indicate the oxygen content of the environment. A higher Ni / Co value indicates a stronger reduction environment.

From the correlation diagram (Fig. 9), the correlation between V/Cr and TOC is good, same trends showed in Ni/Co and TOC correlation (Fig. 10). The results imply that the Wufeng period is a suboxic environment and the early Longmaxi period is a reducing environment. For siliceous shale (Type V), the sedimentary environment is highly reducible and presents a strong reducing sulfidation environment at the bottom of the Longmaxi Formation and turned to be oxidative and shallower upwards. For the dolomitic mudstone (Type IV), the reducing environment is weakened. For the mudstone (Type I), silty mudstone (Type III), and bioclastic limestone (Type II), the sub-oxidized environment indicated the water column is shallower. The Mo and U elements in sediments originated in ocean water. In the anoxic environment, U and Mo were reduced to low U^{+4} and Mo^{+4}, which were easily precipitated and enriched in sediments (Algeo TJ and Tribovillard N et al., 2009; Tribovillard N et al., 2012). The Mo-U covariation diagram also manifests the same trend. According to the enrichment factors diagram of Mo *vs*. U (Fig. 11), siliceous rocks and dolomitic mudstones basically deposited in the reduction-sulfurization reduction zone while the limestone and siltstone basically deposited in the sub-oxidation zone.

5.1.3. Paleo-productivity

Palaeo-productivity is a key factor control the organic matter enrichment in marine sediments. The elements Mn, Zn, Cd, Si, and Ba could be used to indicate the paleo-productivity.

The Longmaxi shale in the study area generally shows high silicon characteristics. As the study area is located in a restricted environment and does not influence rising ocean currents. And according to the silicogenous Al-Fe-Mn ternary diagram (Fig. 12), the siliceous is not hydrothermally generated. Meanwhile, prolific radiolarians, siliceous bio-fossils, and detrital quartz had been found in the thin section identification indicating the siliceous content may be biogenic and detrital generated. Using the excess silicon calculation formula to eliminate debris interference could obtain bio-generated silicon content which can be used as an indicator of paleo-productivity. In addition, according to previous literature studies, Mn enrichment in the study area is mainly affected by biological activities in the carbonate platform area (Tang X et al., 2017). Thus, Mn indicated the paleo-productivity of the limestone in the study area.

Mn, Zn, and Cd showed high productivity in dolomitic mudstones (Type IV, purple belt in Fig. 12) and comparatively high paleo-productivity in mudstone (Type Ⅰ, yellow belt in Fig. 12) and silty mudstone (Type Ⅲ, light brown in Fig. 12). For siliceous shale (Type V, blue belt in Fig. 12), SiO_{2bio} shows high paleo-productivity, while for limestone (Type Ⅱ, grey belt in Fig. 12), Mn showed high paleo-productivity in the study area.

5.2. Organic matter accumulation mechanism

The organic matter enrichment mechanism in black shale

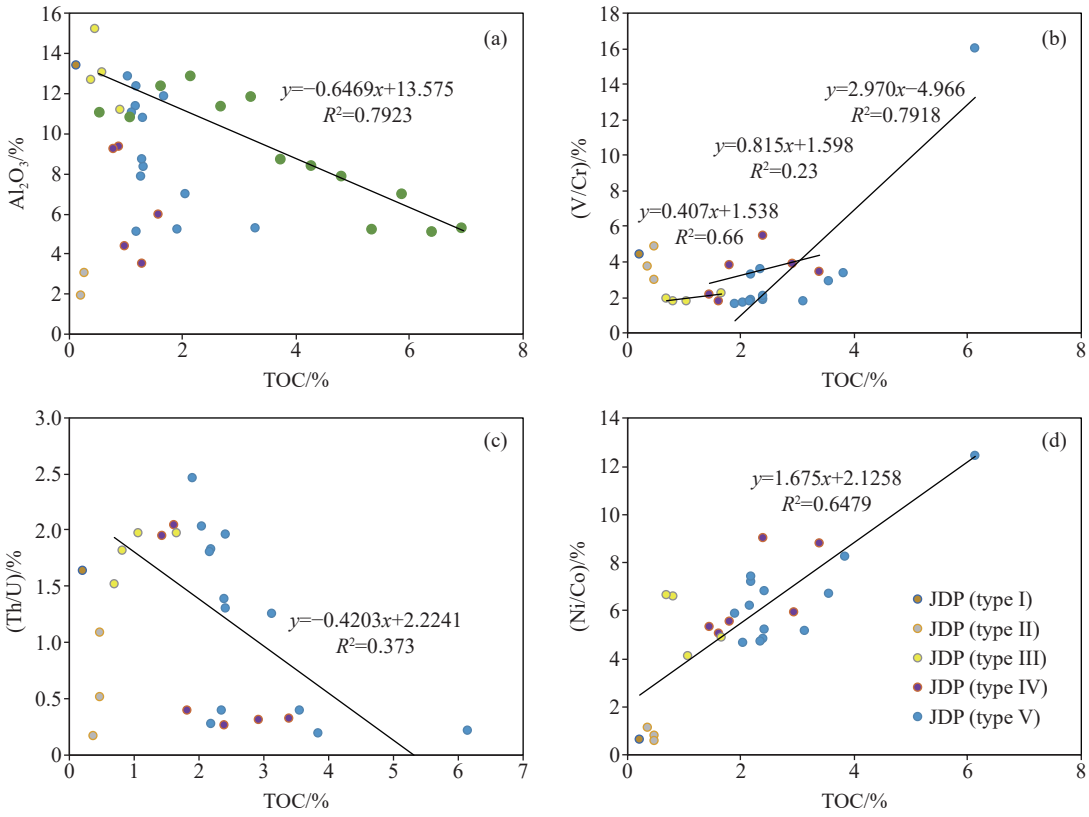

Fig. 10. Relationships of TOC to proxies of redox condition and detrital input.

remains controversial. The discussion focuses on the main determinant of organic matter enrichment. Whether it is mainly controlled by the primary producer or by the organic matter preservation condition which is reducing the sedimentary environment. The organic matter enrichment pattern can be described by using the cross-plot map between

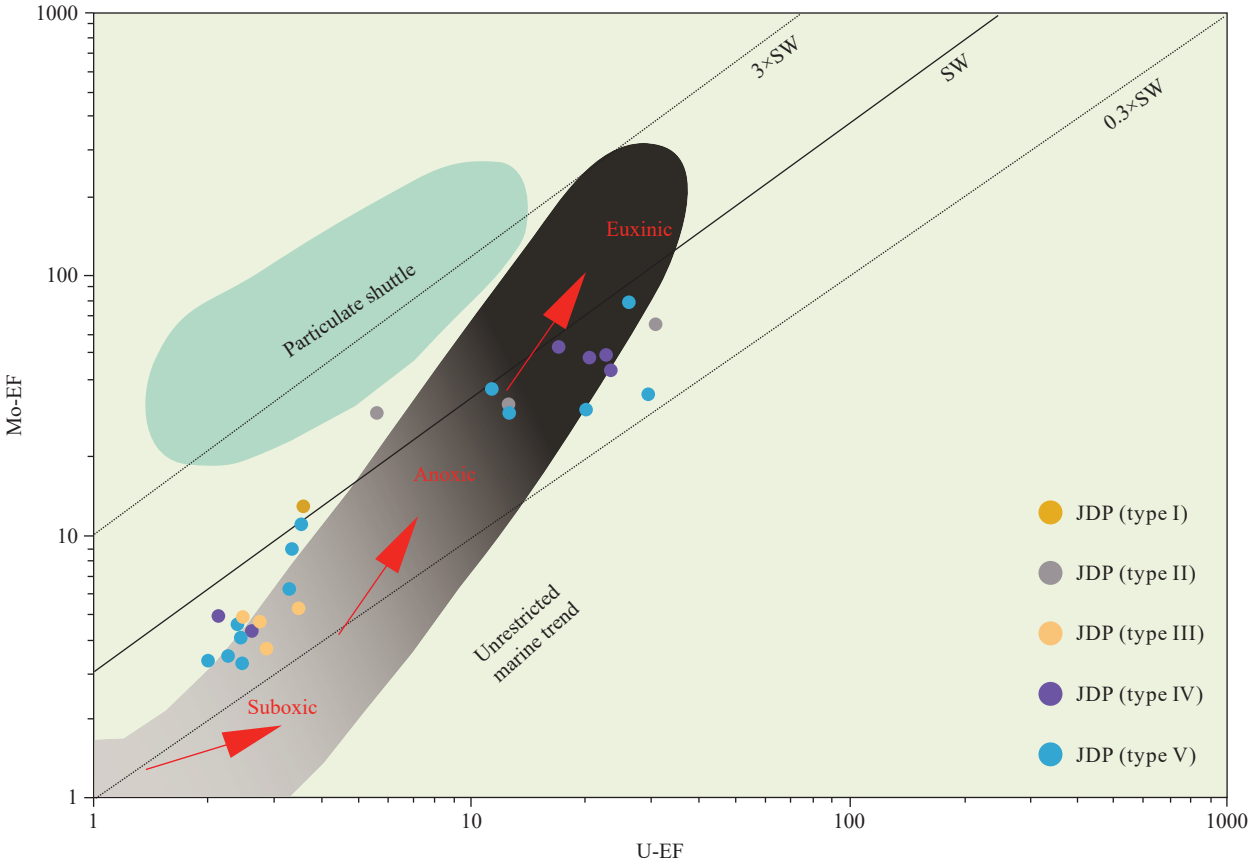

Fig. 11. Enrichment factors (EFs) of Mo *vs.* U. The lines exhibit Mo/U ratios equal to seawater (SW). The patterns of U-EF and Mo-EF are compared to the model of Algeo TJ and Tribovillard N et al., (2009).

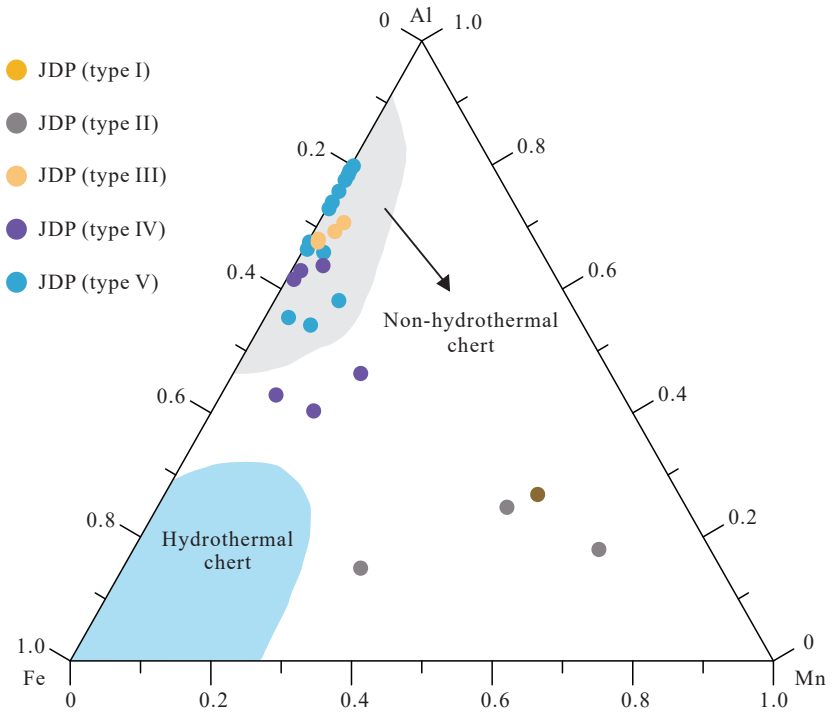

Fig. 12. Crossplots of various geochemical components (A-D) of siliceous content.

the TOC and the terrigenous influx (Al_2O_3), or the paleo-productivity index (Mn, Zn, Ba, SiO_2), or the redox conditions (Ni/Co, Th/U, V/Cr).

As shown in Fig. 9, in the study area, the TOC content is positively correlated with the Ni/Co, and V/Cr ratio, and negatively correlated with the Th/U ratio, indicating that reduction conditions are the controlling factors of organic matter enrichment. And the TOC content is negatively correlated with the detrital proxy (Al_2O_3), which indicates that terrigenous input has a negative influence on organic matter enrichment.

For the relationship between TOC and Paleo-productivity, the SiO_2 and Zn content is positively correlated with TOC, while the Mn or Ba content has no clear relationship with TOC. The results indicated that siliceous organisms are the main contributor to organic enrichment (Fig. 13). This was consistent with prior reports (Wang S et al., 2016; Li YF et al., 2017). Its paleontological flourishing may be related to the abundance of nutrients that are transported by frequent volcanic activities during that period, thus promoting Paleo-productivity.

The Wufeng Formation is in a high-productivity environment, and a large number of organic matter was produced, some of which decompose and deplete oxygen in the water (Wang S et al., 2016), resulting in a hypoxia reduction environment, which makes the remaining organic matter well preserved. The typical lithofacies in the Wufeng Formation is dolomite mudstone (Type Ⅳ). It is mainly characterized by high TOC and high calcium, and the calcium component mainly comes from dolomite. The sedimentary environment is a shallower, weak-reducing environment, and has high paleo-productivity.

In the early stage of the Longmaxi Formation, due to the rise of sea level, the water was deep and the bottom water body had an anoxic reduction environment, which was conducive to the preservation of organic matter. The typical lithofacies in the lower Longmaxi Formation is siliceous mudstone (Type V). It is mainly characterized by high SiO_2 content and high TOC. Its sedimentary water body is a deep-water shelf environment, and the sedimentary environment is a strong reduction-reduction environment with high paleo-productivity.

Therefore, the organic matter enrichment mechanism in Wufeng Formation is dominated by high productivity, while the bottom of the Longmaxi Formation is dominated by hypoxic reduction environment and high Paleo-productivity. The organic-rich lithofacies mainly consists of siliceous shale (type V) and dolomitic mudstone.

5.3. Organic-rich shale development model

Many scholars have noted that both Wufeng Formation and Longmaxi Formation have high productivity and hypoxic reduction conditions, but their development models are different.

During the Early Ordovician Wufeng period, active

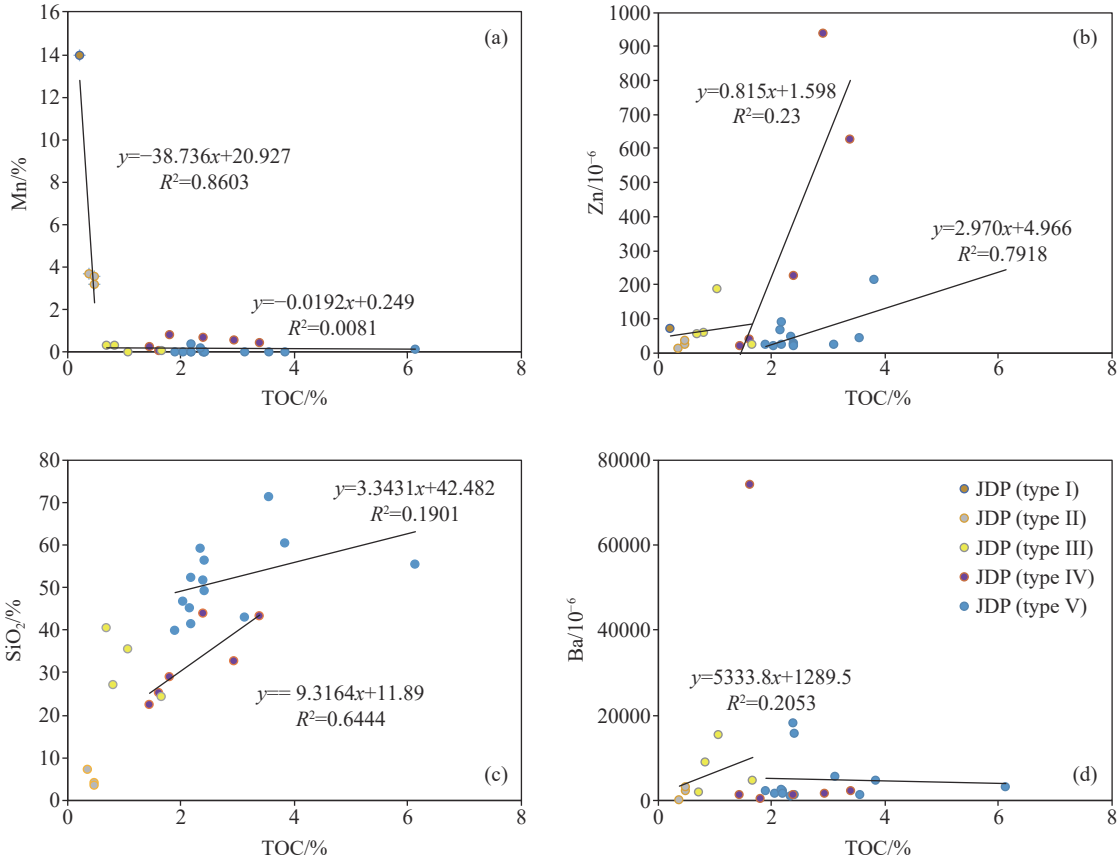

Fig. 13. Relationships of TOC to proxies of paleo-productivity.

volcanic events enriched the nutrients in seawater and resulted in a large amount of organic matter accumulated under the background of high Paleo-productivity. Partial organic matter experienced decomposition and consumed the oxygen in water bodies, depleted the negative effects on the organic matter preservation of the oxidic environment in a shallower water environment, and formed the dolomitic shale with higher organic carbon content. If the paleo-productivity is reduced or the water depth decreased further, resulting in an oxidative environment, the oxygen cannot be fully consumed by organic matter. As a result, the oxidation environment developed, and the carbonate rocks with high calcium content and low carbon content were deposited (type II) (Fig. 14a).

In the Early Silurian Longmaxi period, the restricted environment and the paleo-sea level fluctuation caused the water body stratification and led to the sulfide of the bottom water. While the paleo-productivity level was also high (Fig. 14b), hence, a set of high-carbon and high-silicon mudstone (Type V) was deposited at the bottom of the Longmaxi Formation. Later with the relative decline of global sea level, and gradual transition to the reducing carboxylation environment, a set of high carbon content dolomite and siliceous mudstone (Type IV) was deposited. Finally, as the sea level continues to fall and large quantities of terrigenous input stop the organic matter enrichment. The sedimentary environment converted to the oxic shallow water environment, and no longer be suitable for organic matter enrichment.

Thus, the most important factor for the enrichment of organic matter in the study area is the reduced environment caused by sea level rise and high paleo-productivity. When the sea level is high, the water body stratification caused by oxygen inefficiency is beneficial for organic matter accumulation. When the sea level is relatively lower, a higher

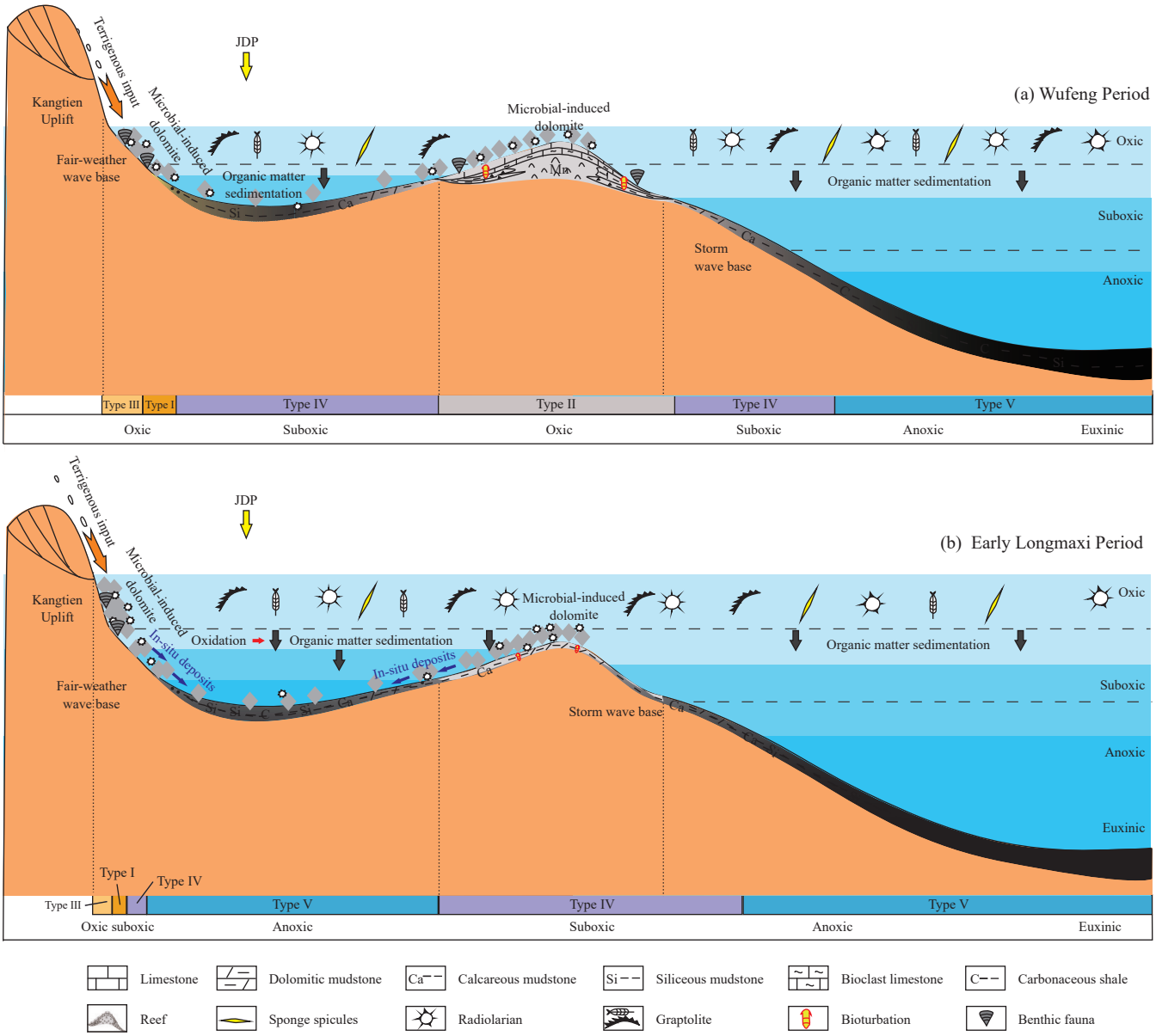

Fig. 14. Diagrammatic sketch illustrating the probable environmental evolution of the Upper Yangtze Basin during the Late Ordovician and Early Silurian.

paleo-productivity could support extra organic matter generated for decomposition, and keep the rest organic matter preserved.

5.4. Shale gas potential assessment

By studying the sedimentary environment and other basic geological conditions of in Wufeng-Longmaxi Formation, the results show that the organic carbon content is relatively high, generally more than 1.0%, and the highest organic carbon content can exceeds 6.0%, and the average content between 1.5 % and 2.5 %. The thickness of organic-rich shale is over 20 m. And the hydrocarbon generation intensity is relatively high. The maturity is moderate, and the *R*o is basically greater than 1.8 %, in the high-over-matured stage of organic matter thermal evolution, indicating that Longmaxi Formation has good resource potential and good exploration prospects in the region.

Meanwhile, the Longmaxi Formation is distributed stable in the area, the dip is relatively gentle. The target shale is covered by the Triassic and Jurassic strata mostly and is only exposed locally around the syncline. The burial depth is generally less than 3000 m according to upper layer thickness calculation. Generally, the organic-rich shale of the Wufeng Formation-Longmaxi Formation is vastly developed in the east of Kangdian Uplift, which is favorable for shale gas accumulation. Hanyuan, Meigu-Mabian area may be a potentially favorable area for shale gas. Thus, the east KangDian Uplift is an important research area for the future exploration of shale gas, and further in-depth research is needed in the future.

6. Conclusions

The key findings of this study are:

(i) Through testing and analysis of outlying shale samples from the Wufeng-Longmaxi Formation in the Hanyuan section on the east KangDian Uplift. Five lithofacies have been defined including mudstone, bioclastic limestone, silty shale, dolomitic shale, and carbonaceous siliceous shale.

(ii) Based on the geochemical characteristics, the detrital influx, redox conditions, and paleo-productivity have been studied as follows: The Wufeng period is a suboxic environment and the early Longmaxi period is a reducing environment. The terrigenous influx gradually increases while the paleo-productivity generally decreases upwards.

(iii) The paleo-environments have been reconstructed and the organic enrichment mechanism has been analyzed. For the area close to the Kangdian Uplift, a restricted area with a water body stratified, bottom water body vulcanized, and the nutrient elements in the seawater were enriched to support a high paleo-productivity due to the volcanic activities, and environment reduction is beneficial to deposit organic-rich shale.

(iv) The high carbonaceous and high siliceous content mudstone (Type V) deposited with high productivity and anoxic environment in the study area is most favorable, and dolomitic and siliceous mudstone (Type IV) deposited in a reductive sub-oxidation environment with high productivity is sub-favorable for organic matter accumulation.

(v) The geological condition and the gas generation capability is favorable in the study area. The TOC is over 2.0% and the thickness is more than 20 m, and *R*o is good, mostly over 1.8 %, and the burial depth is less than 3000 m. These results implied that the east Kangdian Uplift has great potential for shale gas exploration.

CRediT authorship contribution statement

An-kun Zhao and Zi-hui Lei conceived of the presented idea and wrote the manuscript. Dong Wang and Qian Zhang carried out the experiment and analyzed the geochemical proxies. Di Zhang conducted the graptolite observation and zonation. Qian Yu supervise the project and contribute to the final version of the manuscript. Ye-xin Zhou contributes to the stratigraphic column analysis. All authors discussed the results and contributed to the final manuscript.

Declaration of competing interest

The authors declare no conflicts of interest.

Acknowledgment

This research was jointly funded by the National Key Laboratory of Oil and Gas Reservoir Geology and Exploitation (PLC20210104), China Geological Survey (DD20221661), and China National Science and Technology Major Project “Test and Application of Shale Gas Exploration and Evaluation Technology (2016ZX05034004)”. The authors are indebted to Prof. Gang-yi Zhai, Prof. Zhi-qiang Shi, and Prof. Jun Peng for comments and suggestions on this paper. This manuscript has benefited from valuable advice from Dr. You-li Wan and Mr. Wei Sun.

References

Algeo TJ, Tribovillard N. 2009. Environmental analysis of paleoceanographic systems based on molybdenum–uranium covariation. Chemical Geology, 268(3), 211–225. doi: 10.1016/j.chemgeo.2009.09.001.

Bernard S, Horsfield B. 2014. Thermal maturation of gas shale systems. Annual Review of Earth and Planetary Science, 42(1), 635–651. doi: 10.1146/annurev-earth-060313-054850.

Cavelan A, Boussafir M, Rozenbaum O, Laggoun-Défarge F. 2019. Organic petrography and pore structure characterization of low-mature and gas-mature marine organic-rich mudstones: Insights into porosity controls in gas shale systems. Marine and Petroleum Geology, 103, 331–350. doi: 10.1016/j.marpetgeo.2019.02.027.

Caplan ML, Marc Bustin R. 1998. Sedimentology and sequence stratigraphy of Devonian-Carboniferous strata, southern Alberta. BulletinofCanadianPetroleumGeology,46(4),487–514.https://doi.org/10.1306/212f9255-2b24-11d7-8648000102c1865d.

Chen X, Rong JY, Li Y, Boucot AJ. 2004. Facies patterns and geography of the Yangtze region, South China, through the Ordovician and Silurian transition. Palaeogeography, Palaeoclimatology, Palaeoecology, 204(3–4), 353–372. doi: 10.1016/S0031-

0182(03)00736-3.

Chen XJ, Jia LQ, Jia T. 2022. China achieved fruitful results in oil-shale gas-coalbed methane exploration and development in 2021. China Geology, 5(2), 355–356. doi: 10.31035/cg2022031.

Dai JX, Zou CN, Dong DZ, Ni YY, Wu W, Gong DY, Wang YM, Huang SP, Huang JL, Fang CC, Liu D. 2016. Geochemical characteristics of marine and terrestrial shale gas in China. Marine and Petroleum Geology, 76, 444–463. doi: 10.1016/j.marpetgeo.2016.04.027.

Dong DZ, Wang YM, Li XJ, Zou CN, Guan QZ, Zhang CC, Huang JL, Wang SF, Wang HY, Liu HL, Bai WH, Liang F, Lin W, Zhao Q, Liu DX, Qiu Z. 2016. Breakthrough and prospect of shale gas exploration and development in China. Natural Gas Industry B, 3(1), 12–26. doi: 10.1016/j.ngib.2016.02.002.

Fan JX, Chen X. 2007. Preliminary report on the Late Ordovician graptolite extinction in the Yangtze region. Palaeogeography, Palaeoclimatology, Palaeoecology, 245, 82−94. doi: 10.1016/j.palaeo.2006.02.019.

Ge XY, Mou CL, Yu Q, Liu W, Men X, He JL. 2019. The geochemistry of the sedimentary rocks from the Huadi No. 1 well in the Wufeng-Longmaxi formations (Upper Ordovician-Lower Silurian), South China, with implications for paleoweathering, provenance, tectonic setting and paleoclimate. Marine and Petroleum Geology, 103, 646-660. doi: 10.1016/j.marpetgeo.2018.12.040.

Guo X, Liu R, Xu S, Feng B, Wen, T, Zhang T. 2022. Structural deformation of shale pores in the fold-thrust belt: The Wufeng-Longmaxi shale in the Anchang Syncline of Central Yangtze Block. Advances in Geo-Energy Research, 6(6), 515–530. doi: 10.46690/ager.2022.06.08.

Hackley PC, Cardott BJ. 2016. Application of organic petrography in North American shale petroleum systems: A review. International Journal of Coal Geology, 163, 8–51. doi: 10.1016/j.coal.2016.06.010.

Hammes U, Eastwood R, McDaid G, Vankov E, Gherabati SA, Smye K, Shultz J, Potter E, Ikonnikova S, Tinker S. 2016. Regional assessment of the Eagle Ford Group of South Texas, USA: Insights from lithology, pore volume, water saturation, organic richness, and productivity correlations. Interpretation, 4(1), C125–C150. doi: 10.1190/INT-2015-0099.1.

Han C, Jiang ZX, Han M, Wu MH, Lin W. 2016. The lithofacies and reservoir characteristics of the Upper Ordovician and Lower Silurian black shale in the Southern Sichuan Basin and its periphery, China. Marine and Petroleum Geology, 75, 181–191. doi: 10.1016/j.marpetgeo.2016.04.014.

Hao F, Zou HY. 2013. Cause of shale gas geochemical anomalies and mechanisms for gas enrichment and depletion in high-maturity shales. Marine and Petroleum Geology, 44, 1–12. doi: 10.1016/j.marpetgeo.2013.03.005.

Jia AL, Wei YS, Jin YQ. 2016. Progress in key technologies for evaluating marine shale gas development in China. Petroleum Exploration and Development, 43(6), 1035–1042. doi: 10.1016/S1876-3804(16)30120-3.

Knapp LJ, McMillan JM, Harris NB. 2017. A depositional model for organic-rich Duvernay Formation mudstones. Sedimentary Geology, 347, 160–182. doi: 10.1016/j.sedgeo.2016.11.012.

Kuypers MMM, Pancost RD, Nijenhuis IA, Sinninghe Damsté JS. 2002. Enhanced productivity led to increased organic carbon burial in the euxinic North Atlantic basin during the late Cenomanian oceanic anoxic event. Paleoceanography, 17(4), 3-1-3-13. https://doi.org/10.1029/2000PA000569.

Lalonde K, Mucci A, Ouellet A, Gélinas Y. 2012. Preservation of organic matter in sediments promoted by iron. Nature, 483(7388), 198–200. doi: 10.1038/nature10855.

Li SZ , Zhou Z, Nie HK, Zhang LF, Song T, Liu WB , Li HH, XU QC, Wei SY, Tao S. 2022. Distribution characteristics, exploration and development, geological theories research progress and exploration directions of shale gas in china. China Geology, 5(1), 110−135. doi: 10.1016/S2096-5192(22)00090-8.

Li YF, Zhang TW, Ellis GS, Shao DY. 2017. Depositional environment and organic matter accumulation of Upper Ordovician–Lower Silurian marine shale in the Upper Yangtze Platform, South China. Palaeogeography, Palaeoclimatology, Palaeoecology, 466, 252–264. doi: 10.1016/j.palaeo.2016.11.037.

Liu ZH, Algeo TJ, Guo XS, Fan JX, Du XB, Lu YC. 2017. Paleo-environmental cyclicity in the Early Silurian Yangtze Sea (South China): Tectonic or glacio-eustatic control? Palaeogeography, Palaeoclimatology, Palaeoecology, 466, 59−76. doi: 10.1016/j.palaeo.2016.11.007.

Ma YQ, Fan MJ, Lu YC, Guo XS, Hu HY, Chen L, Wang C, Liu XC. 2016. Geochemistry and sedimentology of the Lower Silurian Longmaxi mudstone in southwestern China: Implications for depositional controls on organic matter accumulation. Marine and Petroleum Geology, 75, 291–309. doi: 10.1016/j.marpetgeo.2016.04.024.

Murray RC. 1990. Diagenetic silica stratification in a paleosilcrete, North Texas. Journal of Sedimentary Research, 60(5), 717–720. https://doi.org/10.1306/212F9255-2B24-11D7-8648000102C1865D.

Nitzer SF, Stephenson MH, Davies SJ, Vane CH, Leng MJ. 2016. Significance of sedimentary organic matter input for shale gas generation potential of Mississippian Mudstones, Widmerpool Gulf, UK. Review of Palaeobotany and Palynology, 224, 146–168. doi: 10.1016/j.revpalbo.2015.10.003.

Pan SQ, Zou CN, Yang ZY, Dong DZ, Wang YM, Wang SF, Wu ST, Huang JL, Liu Q, Wang D, Wang ZY. 2015. Methods for shale gas play assessment: A comparison between Silurian Longmaxi shale and Mississippian Barnett shale. Journal of Earth Science, 26(2), 285–294. doi: 10.1007/s12583-015-0524-0.

Tan JQ, Weniger P, Krooss B, Merkel A, Horsfield B, Zhang JC, Boreham CJ, Graas GV, Tocher BA. 2014. Shale gas potential of the major marine shale formations in the Upper Yangtze Platform, South China, Part II: Methane sorption capacity. Fuel, 129, 204–218. doi: 10.1016/j.fuel.2014.03.064.

Tang X, Zhang JC, Liu Y, Yang C, Chen Q, Dang W, Zhao PW. 2017. Geochemistry of organic matter and elements of black shale during weathering in Northern Guizhou, Southwestern China: Their mobilization and inter-connection. Geochemistry, 78(1), 140–151. doi: 10.1016/j.chemer.2017.08.002.

Torsvik T, Cocks L. 2016. Earth History and Palaeogeography. Cambridge, Cambridge University Press. doi: 10.1017/9781316225523.

Tribovillard N, Algeo TJ, Lyons T, Riboulleau A. 2006. Trace metals as paleoredox and paleoproductivity proxies: An update. Chemical Geology, 232(1), 12–32. doi: 10.1016/j.chemgeo.2006.02.012.

Tribovillard N, Algeo T J, Baudin F, Riboulleau AJCG. 2012. Analysis of marine environmental conditions based onmolybdenum–uranium covariation—Applications to Mesozoic paleoceanography. Chemical Geology, 324, 46–58. https://doi.org/10.1016/j.chemgeo.2011.09.009.

Tserolas P, Maravelis AG, Tsochandaris N, Pasadakis N, Zelilidis A. 2019. Organic geochemistry of the Upper Miocene-Lower Pliocene sedimentary rocks in the Hellenic Fold and Thrust Belt, NW Corfu island, Ionian sea, NW Greece. Marine and Petroleum Geology, 106, 17–29. doi: 10.1016/j.marpetgeo.2019.04.033.

Wang S, Dong D, Wang Y, Li X, Huang J, Guan Q. 2016. Sedimentary geochemical proxies for paleoenvironment interpretation of organic-rich shale: A case study of the Lower Silurian Longmaxi Formation, Southern Sichuan Basin, China. Journal of Natural Gas Science and Engineering, 28, 691–699. doi: 10.1016/j.jngse.2015.11.045.

Yuan K, Huang WH, Wang T, Li SZ, Sun XC, Fang XX, Xiao JP, Guo J. 2023. Tectonic evolution and accumulation characteristics of

Carboniferous shale gas in Yadu-Ziyun-Luodian aulacogen, Guizhou Province, South China. China Geology, 6(4), 646–659. doi: 10.31035/cg2022059.

Zhao AK, Shi ZQ, Wang XF, Peng J, Lei ZH, Yu Q, Hao JY, Zhang D. 2022. Characteristics of organic-rich dolomites from upper Ordovician Wufeng Formation —Lower Silurian Longmaxi Formation in the eastern part of Kangdian ancient land and their geological significances. Bulletin of Mineralogy, Petrology and Geochemistry (in Chinese with English abstract), 41(2), 307–316. doi: 10.19658/j.issn.1007-2802.2021.40.105.

Zhao AK, Yu Q, Zhou YX, Lei ZH, Yan JF, Men YP, Zhang Q, Zhang Di. 2021. Analysis and quantitative evaluation of the shale gas preservation conditions in the margin areas of Sichuan Basin. 41(3), 376–386. doi: 10.19826/j.cnki.1009-3850.2021.05003.

Zhao L, Mao W, Liu Z, Cheng S. 2023. Research on the differential tectonic-thermal evolution of Longmaxi shale in the southern Sichuan Basin. Advances in Geo-Energy Research, 7(3), 152–163. doi: 10.46690/ager.2023.03.02.

Zhou L, Algeo T J, Shen J, Hu ZF, Gong HM, Xie SC, Huang JH, Gao S. 2015. Changes in marine productivity and redox conditions during the Late Ordovician Hirnantian glaciation. Palaeogeography, Palaeoclimatology, Palaeoecology, 420, 223–234. doi: 10.1016/j.palaeo.2014.12.012.

Zou CN, Du JH, Xu CC, Wang ZC, Zhang BM, Wei GQ, Wang TS, Yao GS, Deng SH, Liu JJ, Zhou H, Xu A, Yang Z, Jiang H, Gu ZD. 2014. Formation, distribution, resource potential, and discovery of Sinian–Cambrian giant gas field, Sichuan Basin, SW China. Petroleum Exploration and Development, 41(3), 306–325. doi: 10.1016/S1876-3804(14)60036-7.

Zou CN, Yang Z, Dai JX, Dong D, Zhang BM, Wang YM, Deng SH, Huang JL, Liu KY, Yang C, Wei GQ, Pan SQ. 2015. The characteristics and significance of conventional and unconventional Sinian–Silurian gas systems in the Sichuan Basin, central China. Marine and Petroleum Geology, 64, 386–402. doi: 10.1016/j.marpetgeo.2015.03.005.

Zou CN, Zhu RK, Chen ZQ, Ogg JG, Wu ST, Dong DZ, Qiu Z, Wang YM, Wang L, Lin SH, Cui JW, Su L, Yang Z. 2019. Organic-matter-rich shales of China. Earth-Science Reviews, 189, 51–78. doi: 10.1016/j.earscirev.2018.12.002.